ELSEVIER

Thermochimica Acta 314 (1998) 205–212

thermochimica acta

Standard enthalpies of formation of some 3*d*, 4*d* and 5*d* transition-metal stannides by direct synthesis calorimetry

S.V. Meschel*, O.J. Kleppa

The James Franck Institute, The University of Chicago, 5640 S. Ellis Ave, Chicago, IL 60637, USA

Received 14 April 1997; accepted 1 July 1997

Abstract

The standard enthalpies of formation of some 3*d*, 4*d* and 5*d* transition-metal stannides have been measured by high-temperature direct synthesis calorimetry at 1473±2 K. The following results are reported; all in kJ/mol of atoms: Ti_6Sn_5: −(43.4±1.4); V_3Sn: −(21.7±1.4); Zr_5Sn_3: −(71.2±2.5); Nb_3Sn: −(15.2±2.3); Ru_3Sn_7: −(18.7±1.4); $RhSn_2$: −(42.1±2.4); Pd_3Sn: −(57.8±1.9); Hf_5Sn_3: −(49.2±2.1); Ir_5Sn_7: −(15.0±1.9); $IrSn_2$: −(12.9±1.6); PtSn: −(58.8±2.3). The results are compared with some earlier values obtained by calorimetry or derived from emf or vapor-pressure measurements. They are also compared with predicted values from the semi-empirical model of Miedema et al., and with available enthalpies of formation for transition-metal germanides. © 1998 Elsevier Science B.V.

Keywords: Calorimetry; Enthalpies of formation; Thermochemistry; Transition-metal stannides

1. Introduction

During recent years, we have in this laboratory conducted systematic studies of the thermochemistry of transition-metal alloys with elements of the IIIB and IVB columns in the Periodic Table [1]. These investigations have included work on borides, aluminides, silicides and germanides of transition-metal elements. In the course of these studies, we noted that relatively few alloys of the transition metals with tin had been investigated. The available calorimetric enthalpies of formation for the Fe–Sn, Co–Sn, Ni–Sn systems were measured by Predel and Vogelbein [2], for the Pd–Sn system by Bryant et al. [3], for the Ru–Sn system by Perring et al. [4] and for the Pt–Sn system by Ferro et al. [5]. These results show that the alloys have relatively large negative enthalpies of formation, which indicates that there is a fairly strong bonding between the metals and tin. The V–Sn and Nb–Sn systems are of considerable technological interest because of the superconducting properties of the V_3Sn and Nb_3Sn compounds [6,7]. The Zr–Sn system is also of special interest because of the technological use of zirconium stannides in pressurized water reactors [8].

Information regarding the phase diagrams of the stannide systems and on the structures of the considered phases is generally available in the literature [9–19]. However, there is no established phase diagram for the Ir–Sn system. Also, the X-ray diffraction patterns of several of the alloys which we studied were not listed in the ASTM powder diffraction file.

*Corresponding author.

PII S0040-6031(97)00467-X

The published literature offers some values for the enthalpies of formation of Nb_3Sn derived from vapor-pressure measurements [7], and for Pd_3Sn from EMF data [3]. For Ru_3Sn_7 and for PtSn, there are calorimetric values [4,5]. We will compare our results with these data. We will also compare our results with the enthalpy predictions based on the semi-empirical model of Miedema et al. [20].

Finally, we will compare our results with the enthalpies of formation of transition-metal germanides recently studied in this laboratory [21–24]. We will also draw a comparison of the thermochemical behavior of the transition-metal stannides with the behavior of the 3*d*, 4*d* and 5*d* aluminides previously studied by the present authors [25–27].

2. Experimental and materials

The experiments were carried out at 1473±2 K in a single-unit differential microcalorimeter which has been described in an earlier communication from this laboratory [28]. All the experiments were performed under a protective atmosphere of argon gas which was purified by passing it over titanium chips at 1173 K. A BN(boron nitride) crucible was used to contain the samples.

All the materials used were purchased from Johnson Matthey/Aesar, Ward Hill, MA; the purity and particle size of the elements are summarized in Table 1.

The two components were carefully mixed in the appropriate molar ratio, pressed into 4 mm pellets at room temperature and dropped into the calorimeter. In a subsequent set of experiments, the reaction products were dropped into the calorimeter from room temperature to measure their heat contents. Between the two sets of experiments, the samples were kept in a vacuum desiccator to prevent reaction with oxygen or moisture.

Table 1
Reported purity and particle size of the elements used in this study

Element	Purity(%)	Particle size(mesh)
Ti	99.9	−200
V	99.5	−325
Zr	99.9	≈ −80 (filed ingot)
Nb	99.8	−325
Ru	99.95	−325
Rh	99.95	−200
Pd	99.95	−200
Hf	99.6	−325
Ir	99.95	−60
Pt	99.9	−200
Sn	99.999	−100

Calibration of the calorimeter was achieved by dropping weighed 4 mm diameter pellets prepared from 2 mm OD high-purity copper wire from room temperature into the calorimeter at 1473±2 K. The enthalpy of pure copper at this temperature, 42.402 kJ/mol of atoms, was obtained from Hultgren et al. [29]. The calibrations were reproducible to within ±1.2%.

The reacted samples were examined by X-ray powder diffraction to assess their structures and to ascertain the absence of unreacted metals. The results of these analyses were conclusive. Hence, we did not feel the need to check the samples further by X-ray microprobe analysis.

The phase diagram of the Ti–Sn system shows the existence of two congruently melting compounds, Ti_3Sn(m.p. 1943 K) and Ti_6Sn_5 (m.p. 1763 K) [9]. We attempted to prepare both compounds in the calorimeter. The X-ray diffraction patterns showed that the reactions were complete, but that the predominant phase in both cases was Ti_6Sn_5. The X-ray diffraction pattern of the product with the weighed in composition Ti_3Sn indicated that, even in this case, the Ti_6Sn_5 phase was predominant. On the other hand, the pattern of the sample with composition Ti_6Sn_5 showed an essentially single phase with only a minor amount of Ti_5Sn_3 (<3 %). Ti_6Sn_5 has a phase transformation at 1063 K. Our pattern matched the pattern of the low temperature α-Ti_6Sn_5 modification in the ASTM powder diffraction file. The X-ray diffraction patterns showed no unreacted components in any of the two reaction products.

The phase diagram of the V–Sn system shows two peritectically melting compounds, V_3Sn (m.p. approx. 1873 K) and V_2Sn_3 (m.p. 1029 K) [9]. We prepared V_3Sn in the calorimeter. The X-ray diffraction pattern did not match the hexagonal, Ni_3Sn-type structure given in the ASTM powder diffraction file. However, the pattern showed that there was no unreacted V or even V_2Sn_3 present. Pearson indicates that there is another modification of V_3Sn, with the cubic Cr_3Si structure[10]. Since the X-ray diffraction pattern of this structure is not listed in the ASTM powder

diffraction file, we generated it from available unit-cell parameters and the atomic coordinates of the structural prototype Cr_3Si [10]. Our X-ray pattern showed that our reaction product was a mixture of the two modifications, but with no other phases present.

The phase diagram of the Zr–Sn system shows the existence of one congruently melting compound, Zr_5Sn_3 (m.p. 2261 K) [9]. We prepared this compound in the calorimeter. The X-ray diffraction pattern agreed well with the pattern in the ASTM powder diffraction file. The reaction was complete; however, we found a minor amount of a second phase, ≈5% of Zr_5Sn_4. The X-ray diffraction pattern of Zr_5Sn_4 was not listed in the ASTM powder diffraction file. We therefore generated its pattern from available unit-cell parameters and the atomic coordinates of its structural prototype Ti_5Ga_4 [10]. We found no unreacted metal, oxide or other phases present. Abriata et al. report experimental difficulties in preparing this compound from finely powdered components, due to the high oxygen affinity of Zr [12]. We prepared our Zr powder by filing it immediately prior to the preparation of the pellets; the reacted samples were kept in a vacuum desiccator between measurements.

The phase diagram of the Nb–Sn system shows three peritectically melting compounds, Nb_3Sn (m.p. 2403 K), Nb_6Sn_5 (m.p. 1193 K) and $NbSn_2$ (m.p. 1108 K) [9]. We prepared Nb_3Sn in the calorimeter. The X-ray diffraction pattern matched well with the pattern in the ASTM powder diffraction file. There was no evidence for the presence of unreacted Nb or for other phases. The structure of this compound is the cubic Cr_3Si type [10].

The phase diagram of the Ru–Sn system shows one congruently melting phase, Ru_3Sn_7 [9]. The melting point is not listed, but is estimated to be ≈1573 K [9]. We prepared this compound in the calorimeter. The X-ray diffraction pattern matched very well the pattern in the ASTM powder diffraction file, indicating an essentially single phase. We found no unreacted elements or other phases present.

The phase diagram of the Rh–Sn system shows two congruently melting compounds, Rh_2Sn and $RhSn_2$ [9]. The exact melting points of these phases are not known. We attempted to prepare both compounds in the calorimeter. The X-ray diffraction pattern of $RhSn_2$ showed that we had no unreacted Rh present; however, the match with the pattern of the high-temperature modification listed in the ASTM powder diffraction file was not good. We generated the patterns of Rh_2Sn, RhSn and of the the low-temperature modification of $RhSn_2$ using the available unit-cell parameters and the atomic coordinates [10]. Comparing our experimental pattern with the pattern in the ASTM powder diffraction file as well as with the generated patterns, we concluded that our sample was a mixture of the high-temperature and low-temperature modifications of $RhSn_2$. No other phases were present within the limits of the sensitivity of the diffractometer. The X-ray diffraction pattern of our sample with composition Rh_2Sn showed a mixture of phases, the predominant phase being the low-temperature modification of $RhSn_2$.

The phase diagram of the Pd–Sn system shows two congruently melting compounds, Pd_3Sn (reported m.p. 1599 K) and the Gamma phase where X_{Sn}=32.0–37.5% (m.p. 1560 K) [9]. We prepared Pd_3Sn in the calorimeter. We found that these samples were all melted at our calorimeter temperature at 1473 K. The sample was quite malleable; hence, it was difficult to powder the sample for X-ray diffraction analysis. The pattern in the ASTM powder diffraction file did not provide a good match of our experimental pattern. The 2Θ values were all somewhat displaced. The editors of the ASTM powder diffraction file had commented that, in this pattern, there is a poor fit of the *d*-values with the unit cell. We checked our pattern for the presence of Pd, $PdSn_4$, PdSn, Pd_2Sn and Pd_3Sn_2 and found none of these phases within the limits of detectability of the equipment. We generated the pattern of Pd_3Sn from available unit-cell parameters and the atomic coordinates ($AuCu_3$, cubic) [10] and found an excellent match with the experimental pattern.

The phase diagram of the Hf–Sn system shows one congruently melting compound, Hf_5Sn_3 [9]. The melting point is not known. We prepared this compound in the calorimeter. The X-ray diffraction pattern showed that the compound was fully reacted. We checked for the presence of secondary phases such as $HfSn_2$, HfSn and found none; however, we found some Hf_5Sn_4 estimated at 10–15 %.

There is no published phase diagram for the Ir–Sn system. However, the structures of five intermetallic phases are known, namely IrSn, Ir_5Sn_7, $IrSn_2$, Ir_3Sn_7

and $IrSn_4$ [9]. We attempted to prepare IrSn, Ir_5Sn_7 and $IrSn_2$ in the calorimeter. We found no unreacted Ir in any of the samples. The compositions Ir_5Sn_7 and $IrSn_2$ provided the samples which were closest to being single phase. However, each of these compounds showed the presence of 10–12% of a second phase.

The phase diagram of the Pt–Sn system shows the existence of two congruently melting compounds, PtSn (m.p. 1578 K) and Pt_3Sn [9]. The melting point of the latter phase was not listed. We attempted to make both compounds in the calorimeter. The X-ray diffraction pattern of PtSn matched very well with the pattern in the ASTM powder diffraction file. However, the pattern for the composition of Pt_3Sn indicated a mixed phase with nearly 40% of PtSn.

We tried to prepare compounds in the Mo–Sn and Ta–Sn binary systems. These compounds proved to be incompletely reacted at our operating calorimeter temperature of 1473 K. There are no reported compounds in the systems W–Sn, Re–Sn and Os–Sn.

3. Results and discussion

The standard enthalpies of formation of the transition-metal stannides determined in this study were obtained from the difference between the results of two sets of measurements. In the first set, the following reaction takes place in the calorimeter:

$$\mathrm{Tr}\ (s,\ 298\,\mathrm{K}) + m\mathrm{Sn}(s,\ 298\,\mathrm{K}) \rightarrow \mathrm{TrSn}_m\ (s \text{ or } l,\ 1473\,\mathrm{K}) \quad (1)$$

here, m represents the molar ratio Sn/Tr, Tr being the considered transition metal (Ti, V, Zr, Nb, Rh, Ru, Pd, Hf, Ir and Pt) while s denotes solid and l denotes liquid. The reacted pellets were re-used in a subsequent set of measurements to determine their heat contents:

$$\mathrm{TrSn}_m\ (s,\ 298\,\mathrm{K}) \rightarrow \mathrm{TrSn}_m\ (s,\ 1473\,\mathrm{K}) \quad (2)$$

The standard enthalpy of formation is given by:

$$\Delta H_f^0 = \Delta H(1) - \Delta H(2) \quad (3)$$

where $\Delta H(1)$ and $\Delta H(2)$ are the enthalpy changes per mole of atoms in the compound associated with reactions (1) and (2).

The experimental results are summarized in Table 2. The second column shows the melting points of the phases (where known), while the third column indicates the structure type. The heat effects associated with reactions (1) and (2) are given in kJ/mol of atoms as the averages of 5–7 consecutive measurements with the appropriate standard deviations. The last column shows the standard enthalpy of formation of the considered phases. The standard deviations given in the last column also reflect small contributions from the uncertainties in the calibrations. Since our samples of Hf_5Sn_3, Ir_5Sn_7 and $IrSn_2$ contained 10–15% of a second phase, we are reporting the values for

Table 2
Summary of the measured standard enthalpies of formation for some transition-metal stannides studied by direct synthesis calorimetry at 1200°C. Data in kJ/mol of atoms

Compound	M.P. (K)	Structure type	$\Delta H(1)$	$\Delta H(2)$	ΔH_f^0
Ti_6Sn_5	1763	Nb_6Sn_5	−8.9±0.4(5)	34.5±1.3(6)	−43.4±1.4
V_3Sn	1873	Cr_3Si	16.6±0.7(7)	38.3±1.2(6)	−21.7±1.4
Zr_5Sn_3	2261	Mn_5Si_3	−36.0±2.2(6)	35.2±1.2(6)	−71.2±2.5
Nb_3Sn	2403	Cr_3Si	17.5±1.7(7)	32.7±1.6(5)	−15.2±2.3
Ru_3Sn_7	?	Ir_3Ge_7	15.7±0.7(6)	33.8±1.2(6)	−18.1±1.4 [b]
			14.4±1.3(5)	33.1±1.2(5)	−18.7±1.8 [b]
$RhSn_2$	?	$CuAl_2$	8.3±1.4(6)	50.4±2.0(5)	−42.1±2.4
Pd_3Sn	1599	Cu_3Au	−26.8±1.2(6)	31.0±1.5(5)	−57.8±1.9
Hf_5Sn_3 [a]	?	Mn_5Si_3	−17.0±1.8(5)	32.2±1.1(9)	−49.2±2.1
Ir_5Sn_7 [a]	?	Co_5Ge_7	15.6±1.4(6)	30.6±1.3(5)	−15.0±1.9
$IrSn_2$ [a]	?	CaF_2	19.5±1.3(6)	32.4±1.0(5)	−12.9±1.6
PtSn	1578	NiAs	−28.3±1.5(5)	30.5±1.8(6)	−58.8±2.3

[a] Indicative results.
[b] These values were obtained using two different Ru samples of slightly different purity.

Table 3
Comparison of the measured standard enthalpies of formation with some experimental data reported in the literature and with predicted values from the semi-empirical model of Miedema et al [20]. Data in kJ/mol of atoms

Compound	ΔH_f^0 (exp), this study	ΔH_f^0 (exp), literature	Method	ΔH_f^0 (pred)
Ti_6Sn_5	−43.4±1.4	−64.4	Calorimetry [30]	−52
V_3Sn	−21.7±1.4	—	—	−16
Zr_5Sn_3	−71.2±2.5	—	—	−81
Nb_3Sn	−15.2±2.3	−16.2	Vapor pressure [7] 1261–2076 K	−16
Ru_3Sn_7	−18.7±1.4	−29.8±0.8 [b]	Calorimetry [4], 1173 K	−9
$RhSn_2$	−42.1±2.4	—	—	−28
Pd_3Sn	−57.8±1.9	−58.6±2.2	Calorimetry [3]	−52
Hf_5Sn_3	−49.2±2.1 [a]	—	—	−70
Ir_5Sn_7	−15.0±1.9 [a]	—	—	−24
$IrSn_2$	−12.9±1.6 [a]	—	—	−20
PtSn	−58.8±2.3	−58.6±2.1	Calorimetry [5]	−57

[a] Indicative values.
[b] Reference state of Sn is Sn(l); value corrected for Sn(s) is −24.9 kJ/mol of atoms (see p. 9).

these compounds as indicative. In the measurements of the heat of formation of Ru_3Sn_7, we used three different samples of Ru all of which were purchased from Johnson Matthey/Aesar Corp. In two of the three samples, the X-ray diffraction pattern of the Ru metal showed ca. 1–2% impurity, even though the material was rated as 99.95% pure. The third sample was free of impurities within the limits of detectability of the diffractometer. The values in Table 2 report the results obtained using the two best Ru samples.

In Table 3, we compare the standard enthalpies of formation reported in the present study with some experimental values from the published literature and with predicted values from the semi-empirical model of Miedema et al. [20]. The earlier heat-of-formation values have been derived from EMF data, from vapor-pressure measurements and for Ti_6Sn_5, Ru_3Sn_7, Pd_3Sn and PtSn by calorimetry. Our results for the heats of formation of Nb_3Sn, Pd_3Sn and PtSn compare well with the values reported by Schiffman and Bailey [7], Bryant et al. [3] and Ferro et al. [5], respectively. However, our result for the enthalpy of formation of Ti_6Sn_5 differs very significantly from the calorimetric value reported by Savin [30]; this value was regarded by the author as an estimate. Our enthalpy of formation value for Ru_3Sn_7 is somewhat lower than the measurement by Perring et al. [4]. The reference state in that study is stated to be the pure metals at the reaction temperature, which means Sn(l). The heat of fusion of Sn at the melting point (506.06 K) is 7.03 kJ/mol of atoms [29]. If we make the usual assumption that the heat of fusion of the pure metal does not vary with temperature, we can adjust the heat of formation reported by Perring et al. for the contribution of the heat of fusion. This will make the value 4.9 kJ/mol of atoms less exothermic, i.e. −24.9 kJ/mol of atoms for Sn(s) at 1173 K. Our value refers to 298 K. It is also worth noting that Miner et al. [31] measured the enthalpy of formation of $RhSn_4$ by tin-solution calorimetry at 700–775 K. Their value, −38.0±2.6 kJ/mol of atoms, is roughly comparable with our value if we assume a simple $X(1-X)$ concentration dependence of the enthalpies, even though the two temperatures are quite different.

Table 3 shows that the predicted enthalpies of formation are in reasonable agreement with our measurements for V_3Sn, Nb_3Sn, Pd_3Sn and PtSn. However, for Ti_6Sn_5, Zr_5Sn_3, Hf_5Sn_3, Ir_5Sn_7 and $IrSn_2$, the predicted values are significantly more exothermic. On the other hand, for Ru_3Sn_7 and $RhSn_2$, they are more endothermic than our experimental results.

In Fig. 1, we present a systematic graph which shows the standard enthalpies of formation of 3*d*, 4*d* and 5*d* transition-metal stannides plotted against the atomic numbers. For the 3*d* stannides, the enthalpy of formation of Sc_5Sn_3 was reported previously by the present authors [32], the value for Mn_2Sn was derived from emf measurements by Lukashenko et al. [33], while the values for FeSn, CoSn and Ni_3Sn were determined via calorimetry by Predel and Vogelbein

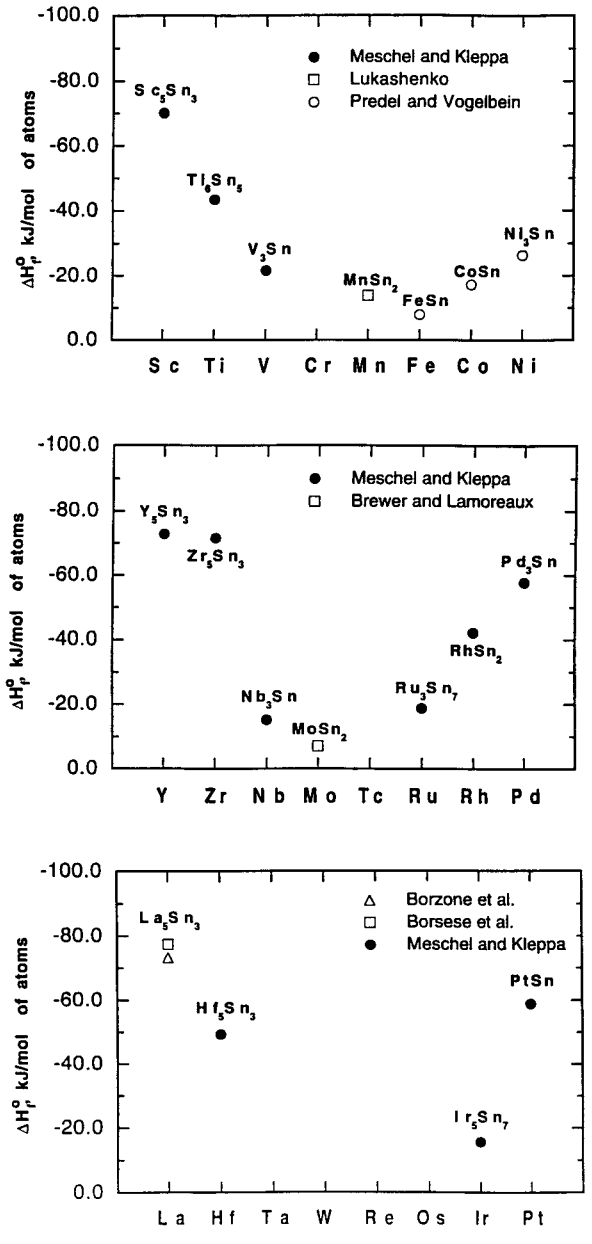

Fig. 1. Standard enthalpies of formation of some 3*d*, 4*d* and 5*d* transition-metal stannides. Data in kJ/mol of atoms.

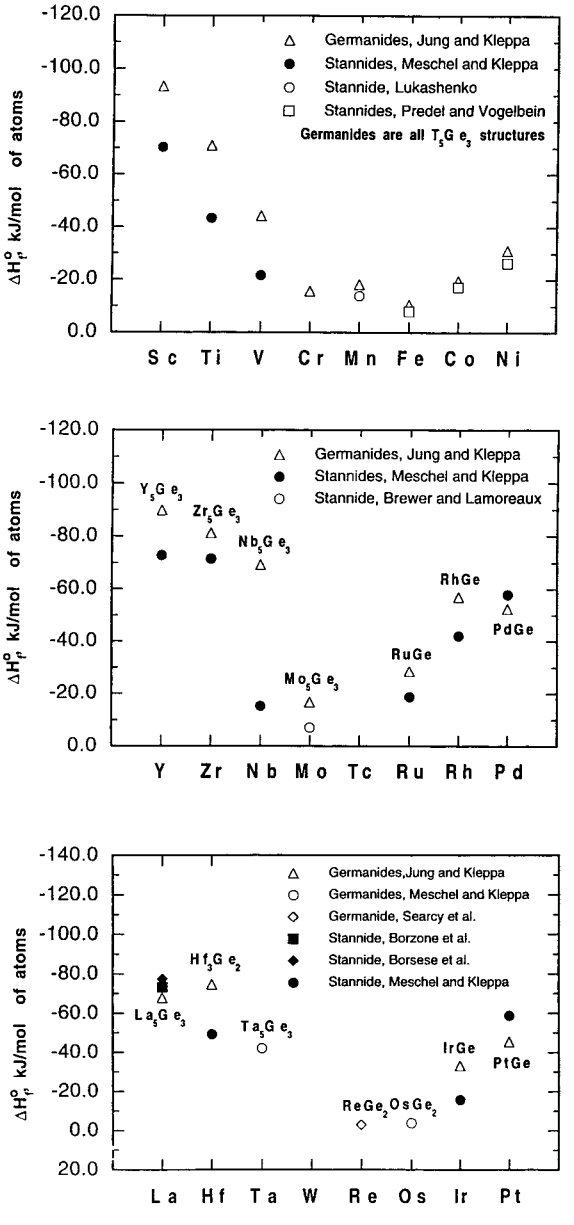

Fig. 2. Comparison of standard entalpies of formation of 3*d*, 4*d* and 5*d* transition-metal stannides with similar transition-metal germanides. The molar composition of the stannides is given in Fig. 1.

[2]. For the 4*d* stannides, the value for the heat of formation of Y_5Sn_3 was reported by the present authors [32], while the plotted value for Mo_3Sn_2 was assessed by Brewer and Lamoreaux [34]. For the 5*d* stannides, the values for the heat of formation of La_5Sn_3 were measured calorimetrically by Borzone et al. [35] and by Borsese et al. [36]. Fig. 1 shows that the enthalpies of formation of the 3*d*, 4*d* and 5*d* stannides all exhibit a roughly parabolic relationship when they are plotted against the atomic number of the transition

Table 4
Comparison of the standard enthalpies of formation of some 3*d*, 4*d* and 5*d* transition-metal stannides and germanides. Data in kJ/mol of atoms

Element	ΔH_f^0 (stannides)	Molar ratio Tr/Sn	ΔH_f^0 (germanides)	Molar ratio Tr/Ge
Ti	−43.5	6 : 5	−70.8	5 : 3
Zr	−71.2	5 : 3	−81.1	5 : 3
Hf	−49.2	5 : 3	−74.6	3 : 2
Co	−15.0	1 : 1	−19.6	5:3
Rh	−42.1	1 : 2	−56.9	1 : 1
Ir	−15.0	5 : 7	−33.1	1 : 1
Ni	−25.0	3 : 2	−31.1	5 : 3
Pd	−57.8	3 : 1	−46.5	1:1
Pt	−58.8	1 : 1	−45.4	1 : 1

metal. The values are most exothermic for the first member of each transition-metal series. We found a similar systematic relationship for the 3*d*, 4*d* and 5*d* aluminides reported in previous communications [25–27]. However, for the lanthanide stannides, the values are nearly constant when plotted against the atomic number of the lanthanide element [32,37].

In Fig. 2, we present a comparison of the standard enthalpies of formation of transition-metal stannides and germanides. Most of the plotted values for the heats of formation of the transition-metal germanides were measured calorimetrically by Jung and Kleppa [21–23]. The enthalpies of formation of Ta_5Ge_3 and $OsGe_2$ were determined by the present authors [24], while the value for $ReGe_2$ is cited from Searcy et al. [37]. Fig. 2 shows that the systematic relationships for the stannides and the germanides are very similar, i.e. roughly parabolic for the 3*d*, 4*d* and 5*d* alloys when plotted against the atomic number of the transition metal. In most cases, the heats of formation of the transition-metal germanides are more exothermic than the stannides. Notable exceptions to this general observation are the compounds of Pd, La and Pt, where we see a reversal, i.e. the stannides are more exothermic than the germanides. For comparison, the enthalpies of formation of the lanthanide germanides are also always more exothermic than the corresponding stannides [32].

In order to see systematic changes among 3*d*, 4*d* and 5*d* triads, we selected the three groups TiZrHf, CoRhIr and NiPdPt; these were the only triads for which the standard enthalpies of formation were available for all three germanide and stannide members of the group. Table 4 shows that, in general, the 4*d* compounds have the most exothermic enthalpies of formation; the heats of formation of the corresponding 3*d* and 5*d* alloys usually have less exothermic values. We observed a similar pattern for the 3*d*, 4*d* and 5*d* aluminides in earlier communications [25–27].

Acknowledgements

This investigation has been supported by the Department of Energy under Grant DE-FGO2-88ER4563, and has also benefitted from the MRSEC facilities at the University of Chicago. We are indebted to Dr. Joseph Pluth for his help with generating the X-ray diffraction patterns from the reported unit-cell parameters and the atomic coordinates.

References

[1] O.J. Kleppa, J. Phase Equil. 15 (1994) 240.
[2] B. Predel, W. Vogelbein, Thermochim. Acta 30 (1979) 201.
[3] A.W. Bryant, W.G. Bugden, J.N. Pratt, Acta Met. 18 (1970) 101.
[4] L. Perring, P. Feschotte, F. Bussy, J.C. Gachon, J. Alloys Compounds 245 (1996) 157.
[5] R. Ferro, R. Cappelli, A. Borsese, S. Delfino, G.B. Bonino, Rendiconti Sci. Fis. Mat. e Nat. Accad. Naz. dei Lincei 54 (1973) 80.
[6] J.F. Smith, Bull. Alloy Phase Diagr. 2 (1981) 210.
[7] R.A. Schiffman, D.M. Bailey, High Temp. Sci. 15 (1982) 165.
[8] Y.U. Kwon, J.D. Corbett, Chem. Materials 2 (1990) 27.
[9] T.B. Massalski, H. Okamoto, P.R. Subramanian, L. Kaczprzak (Eds.), Binary Alloy Phase Diagrams, ASM, Metals Park, OH, 2nd edn., 1990.

[10] P. Villars, L.D. Calvert (Eds.), Pearson's Handbook of Crystallographic Data for Intermetallic Phases, ASM, Metals Park, OH, 1985.
[11] D.J. McPherson, M. Hansen, Trans. ASM 45 (1953) 915.
[12] J.P. Abriata, J.C. Bolcich, D. Arias, Bull. Alloy Phase Diagr. 4 (1983) 147.
[13] H. Okamoto, J. Phase Equil. 12 (1991) 472.
[14] H. Nowotny, H. Auer-Welsbach, J. Bruss, A. Kohl, Monatsh. Chem. 90 (1959) 15.
[15] E.E. Havinga, H. Damsma, P. Hokkeling, J. Less-Common Metals 27 (1972) 169.
[16] S. Heinrich, K. Schubert, J. Less-Common Metals 52 (1977) 87.
[17] I.R. Harris, G.V. Raynor, C.J. Winstanley, J. Less-Common Metals 12 (1967) 69.
[18] W. Rieger, H. Nowotny, F. Benesovsky, Monatsh. Chem. 96 (1965) 233.
[19] H. Boller, H. Nowotny, A. Wittmann, Monatsh. Chem. 91 (1960) 1174.
[20] F.R. deBoer, R. Boom, W.C.M. Mattens, A.R. Miedema, A.K. Niessen, Cohesion in Metals. Transition Metal Alloys., Elsevier Sci. Publ., Amsterdam, 1989.
[21] W.G. Jung, O.J. Kleppa, J. Less-Common Metals 169 (1991) 85.
[22] O.J. Kleppa, W.G. Jung, High Temp. Sci. 29 (1990) 109.
[23] W.G. Jung, O.J. Kleppa, J. Less-Common Metals 169 (1991) 93.
[24] S.V. Meschel, O.J. Kleppa, J. Alloys Compounds 216 (1994) L13.
[25] S.V. Meschel, O.J. Kleppa, J. Alloys Compounds 191 (1993) 111.
[26] S.V. Meschel, O.J. Kleppa, J. Alloys Compounds 197 (1993) 75.
[27] S.V.Meschel, O.J. Kleppa, J.S. Faulkner, R.G. Jordan (Eds.), Metallic Alloys: Experimental and Theoretical Perspectives., Kluwer Acad. Publ., The Netherlands 1994, pp. 103–112.
[28] O.J. Kleppa, L. Topor, Thermochim. Acta 139 (1989) 291.
[29] R. Hultgren, P.D. Desai, D.T. Hawkins, M. Gleiser, K.K. Kelley, D.D. Wagman, Selected Values of the Thermodynamic Properties of the Elements, ASM, Metals Park, OH, 1973, p. 154.
[30] V.D. Savin, Russ. J. Phys. Chem. 47 (1973) 1423.
[31] R.V. Miner Jr., P.J. Spencer, M.J. Pool, Trans. Met. Soc. AIME 242 (1968) 1553.
[32] S.V. Meschel, O.J. Kleppa, J. Alloys Compounds 238 (1996) 180.
[33] G.M. Lukashenko, R.I. Polotskaya, K.A. Dyuldina, Russ. Metall. 4 (1972) 150.
[34] L. Brewer, R.H. Lamoreaux, Atomic Energy Review, L. Brewer (Ed.), Special Issue #7, Vienna, 1980, pp. 106–7.
[35] G. Borzone, A. Borsese, R. Ferro, Z. Anorg. Allg. Chem. 501 (1983) 199.
[36] A. Borsese, G. Borzone, R. Ferro, J. Less-Common Metals 70 (1980) 213.
[37] A.W. Searcy, R.A. McNees Jr., J.M. Criscone, J. Amer. Chem. Soc. 76 (1954) 5287.